Inflammatory Signals Enhance Piezo2-Mediated Mechanosensitive Currents

Adrienne E. Dubin[1], **Manuela Schmidt**[1,3], **Jayanti Mathur**[2], **Matthew J. Petrus**[2], **Bailong Xiao**[1], **Bertrand Coste**[1], and **Ardem Patapoutian**[1,2]

[1]Department of Cell Biology, The Scripps Research Institute (TSRI), La Jolla, CA 92037, USA

[2]Genomic Institute of the Novartis Research Foundation (GNF), San Diego, CA 92121, USA

Summary

Heightened nociceptor function caused by inflammatory mediators such as bradykinin contributes to increased pain perception (hyperalgesia) to noxious mechanical and thermal stimuli. While sensitization of the heat transducer TRPV1 largely subserves thermal hyperalgesia, cellular mechanisms underlying mechanical hyperalgesia have been elusive. The role of the mechanically-activated (MA) channel piezo2 (known as FAM38B) present in mammalian sensory neurons is unknown. We test the hypothesis that piezo2 activity is enhanced by bradykinin, an algogenic peptide that induces mechanical hyperalgesia within minutes. Piezo2 current amplitude is increased and inactivation slowed by bradykinin 2 receptor (BDKRB2) activation in heterologous expression systems. Protein Kinase A (PKA) and Protein Kinase C (PKC) agonists enhance piezo2 activity. BDKRB2-mediated effects are abolished by PKA and PKC inhibitors. Finally, piezo2-dependent MA currents in a class of native sensory neurons are enhanced 8-fold by bradykinin via PKA and PKC. Thus, piezo2 sensitization may contribute to PKA- and PKC-mediated mechanical hyperalgesia.

Introduction

There is accumulating evidence that enhanced pain to noxious mechanical stimuli at sites of inflammation (primary hyperalgesia) is due to peripheral sensitization of mechanotransduction in nociceptors (Hucho and Levine, 2007; Woolf and Ma, 2007). Cellular mechanisms underlying thermal hyperalgesia involve sensitization of the heat transducer TRPV1 (Huang et al., 2006). Although a variety of signaling pathways contribute to the development and maintenance of mechanical hyperalgesia (Hucho and Levine, 2007; Woolf and Ma, 2007), molecular mechanisms leading to peripheral sensitization of nociceptors have remained elusive (Lewin and Moshourab, 2004; Tsunozaki and Bautista, 2009; Woolf and Ma, 2007). The recently discovered MA ion channels piezo1 (known as FAM38A) and piezo2 (known as FAM38B) (Coste et al., 2010; Coste et al., 2012) are expressed in mammalian skin and sensory dorsal root ganglia (DRGs) (Coste et al., 2010). Piezo2 is expressed in both myelinated and unmyelinated DRG neurons, some of which co-express the nocisensor TRPV1 (Coste et al., 2010), and therefore could play a role in

mechanotransduction of noxious stimuli. Indeed, the piezo protein in Drosophila contributes to mechanical nociception (Kim et al., 2012). If mammalian piezo2 also plays a role in mechanical hyperalgesia during inflammation, then its mechanical responses could be enhanced in response to inflammatory signals. The potent algogenic peptide bradykinin (BK) plays an important role in acute mechanical hyperalgesia observed after inflammation largely through its activation of BDKRB2 G protein coupled receptors and downstream signaling pathways which include PKA and PKC (Burgess et al., 2000; Leeb-Lundberg et al., 2005; Mizumura et al., 2009; Steranka et al., 1988). We tested the hypothesis that BDKRB2 activation enhances piezo2 activity. We find that piezo2-dependent currents are dramatically increased in amplitude and inactivation slowed by activation of BDKRB2 in both heterologous expression systems and native sensory neurons through a mechanism that involves PKA and PKC.

Results and Discussion

We first tested whether recombinant piezo2 could be modulated by intracellular signaling pathways mobilized by BDKRB2 activation. Piezo2-mediated currents were elicited by poking transiently transfected HEK293T cells with a blunt glass probe (Coste et al., 2010; McCarter et al., 1999). Recombinant piezo2 and BDKRB2 were co-transfected together with GFP to identify transfected cells ("Piezo2+BDKRB2-HEK"). BDKRB2 activation by 300nM BK robustly increased the amplitude of piezo2-mediated MA currents and slowed inactivation (τ-inac) (Figure 1A, red traces). The area under the curve (AUC; see Experimental Procedures) indicating the net ion flux during mechanical stimulation was enhanced 6.5-fold by BK compared to vehicle-treated cells (Figure 1B). The kinetics of MA currents in naïve Piezo2+BDKRB2-HEK cells were similar to those expressing piezo2 alone ("Piezo2-HEK") (5.0 ± 0.2 msec (n=133) and 4.7 ± 0.2 msec (n=124), respectively) revealing little or no constitutive BDKRB2 activity. Piezo2 activity was not influenced by BK (1μM) in the absence of BDKRB2 expression (data not shown). Exogenous BDKRB2 activation enhanced piezo2 currents in other cell lines (e.g., F-11 cells) (data not shown). To determine whether BK could have long lasting effects on piezo2 currents, we recorded from Piezo2+BDKRB2-HEK cells pre-exposed to BK and compared their MA currents to those in control cells never exposed to BK; MA currents from cells pre-exposed to $0.3–1\mu$M BK revealed longer decay times (τ-inac $=12.1\pm1.6$ msec, n=9) compared to naïve cells (5.4 ± 0.4 msec, n=20; P<0.005) suggesting a long-lasting modulation in intact cells. BK-induced increases in amplitude and τ-inac were similarly dependent on the BK concentration with EC_{50} ~25nM (Figure 1C) as expected for a requirement of BDKRB2 activation (Leeb-Lundberg et al., 2005; Mizumura et al., 2009). Exposure of Piezo2+BDKRB2-HEK cells to BK produced a small inward (-185 ± 35pA at -80mV; n=25) with a latency of 34 ± 3sec (n=25), but there was no correlation between MA I_{max} and BK-induced holding current suggesting piezo2 was not directly activated by BDKRB2 activation (data not shown). The estimated latency for the BK-induced enhancement of piezo2 (determined during application of a constant stimulus (at ~25% of I_{max}) every 5 sec) was 52 ± 5 sec (n=16)). Exogenous BDKRB2 were required for the enhancement of piezo2-mediated MA currents since the specific BDKRB2 antagonist HOE-140 blocked the BK effect on piezo2 currents (Figure 1D, "BK+HOE-140"). HOE-140 exposure had no effect on naïve piezo2-mediated currents in Piezo2+BDKRB2-HEK cells (data not shown) consistent with lack of constitutive BDKRB2 activity. Changes in both piezo2 current amplitude and τ-inac required G protein activation since inclusion of GDPβS (667μM) in the pipette occluded both effects on amplitude and τ-inac (Figure 1D, "BK+GDPβS"). Furthermore, intracellular GTPγS (500μM) enhanced MA amplitude, τ-inac and AUC of piezo2 over 3 to 25min compared to vehicle controls (Figure 1E). After 30min in G protein $\beta\gamma$ inhibitor gallein (30μM), piezo2 currents were still effectively increased by BK in the continued presence of gallein

indicating a major role for G protein α subunits (ampl: 2.0±0.2-fold (p<0.05 compared to changes in the presence of vehicle); τ-inac: 1.7±0.1-fold, p<0.05).

Since BDKRB2 can couple to Gαs, Gαq, Gαi and Gαo, we pharmacologically assessed the role of intracellular signaling pathways regulated by these G proteins. Since roles for PKA and PKC are known in mechanical hyperalgesia (Bhave and Gereau, 2004; Hucho and Levine, 2007), we tested whether agonists of these kinases could enhance recombinant piezo2 currents. We assessed the potential role of the cAMP/PKA pathway using the membrane permeable analog of cAMP, 8-BrcAMP, to directly activate PKA. Exposure of cells to 100–300μM 8-BrcAMP increased amplitude, τ-inac and AUC (Figure 2A, rose bars). The PKC activator PMA (1μM) was similarly effective (Figure 2A, green bars) while the inactive congener 4αPMA had no effect (hatched bars). A combination of 8-BrcAMP and PMA had no apparent additive effect (Figure 2A, brown stippled bars). An example of MA currents reversibly modulated by both agonists is shown in Figure 2B. The PKA inhibitor H-89 (10μM) and PKC inhibitor BIM I (1μM) applied together effectively abrogated the BK-induced changes in both parameters (Figure 2C, brown bars) whereas antagonists applied alone were significantly less, if at all, effective (Figure 2C), suggesting either PKA or PKC pathway is capable of similarly modulating piezo2.

BK increases intracellular calcium largely through activation of the Gαq pathway (Leeb-Lundberg et al., 2005; Mizumura et al., 2009). We tested whether PLC and/or intracellular calcium were required for BK modulation of piezo2. No enhancement of piezo2-mediated currents was observed during 4–5min exposure to the PLC activator m-3M3FBS (Bae et al., 2003) (25μM), suggesting PI-PLC pathways do not increase piezo2 activity (Figure S1; hatched bars). In the same heterologous system and under the same recording conditions, m-3M3FBS enhanced TRPA1 channel activity with a latency of 30–45sec (data not shown) consistent with PLC-dependent activation of TRPA1 (Dai et al., 2007). Consistent with the inability of the PI-PLC activator to modulate piezo2, inhibition of PI-PLC isoforms by U73122 (Bleasdale et al., 1990) or Et-18-OCH3 (edelfosine) (Powis et al., 1992) for up to 3 hours had no effect on BK-induced changes (Figure S1), although both inhibitors effectively blocked BK-induced uncoupling of clustered HEK293T cells compared to controls including inactive U73343 (Hofgaard et al., 2008; van Zeijl et al., 2007) (data not shown). Inhibition of store release by thapsigargin (1μM) also had no effect on BK-induced changes in piezo2 currents (Figure S1), consistent with previous work on rapidly adapting (RA) currents in DRG neurons (Rugiero et al., 2010) (AED, unpublished work) that are largely mediated by piezo2 (Coste et al., 2010). Since BK is known to activate Gαo (an activator of PC-PLC (Kennedy et al., 1996)), we investigated the role of PC-PLC using the Gαi/Gαo inhibitor pertussis toxin (PTX; 100–200ng/ml, 6–24hr) and the PC-PLC inhibitor D609 (100μM, 15min). Neither agent reduced the BK-induced enhancement although PKA inhibitors were not included in these studies (Figure S1 and data not shown). Long exposures to PTX, U73122, edelfosine, thapsigargin and D609 had no effect on initial piezo2 amplitude or τ-inac values (Table S1).

We next sought to determine whether piezo2 expressed in native sensory neurons could be sensitized by BK. We have previously shown that ~20% of cultured adult DRG neurons express RA MA currents and this population is largely reduced by piezo2 RNAi treatment (Coste et al., 2010). However, since specific markers for this population are unavailable, we tested whether RA MA currents might be enriched in a morphologically distinct population and whether these currents were dependent on piezo2. Rosette neurons have been reported to express RA MA currents (Coste et al., 2007; Dubreuil et al., 2004) and are identifiable after 16hr when cultured with the BDNF receptor agonist NT-4 (Lindsay, 1988) together with NGF. Although some Rosette neurons displayed RA MA currents, their τ-inac ranged from 2 to 54 msec (τ-inac =15±2 msec, n=25). We then screened neurons having distinctive

morphologies (e.g., neurons with flattened processes or neurons with extremely long, thin branching processes essentially lacking varicosities) for a population expressing RA currents similar to those mediated by heterologously expressed piezo2. Remarkably, >95% of a population of small-medium neurons (soma diameter: $27\pm1\mu m$, n=73; C_m: $49\pm2pF$, n=96) with flattened processes (Figure 3A) and similar incidence as Rosettes (~2–5% of cultured neurons; data not shown) displayed RA MA currents (τ-inac =6.3±0.4msec; n=95). We dubbed these neurons "Inkblots" (see criteria in Experimental Procedures). Although medium diameter RA MA fibers are generally considered non-nociceptive, both C- and Aδ fibers with RA responses encoding mechanical stimuli into the noxious range have been reported (Andrew and Greenspan, 1999; Boada and Woodbury, 2007; Potenzieri et al., 2008). Naïve Inkblots revealed prolonged action potential (AP) durations (3.1±0.3msec, n=33) and sensitivity to capsaicin (five of 5 Inkblots tested revealed an increase in conductance to 1μM capsaicin (45±25nS, range 3–113nS; C_m: 60±15pF)), consistent with their being nociceptors (Djouhri et al., 1998). Nucleofection of neuronal cultures with siRNA directed to piezo2 (Coste et al., 2010) selectively decreased the MA current density in these neurons compared to scrambled siRNA controls (Figure 3B, grey bars), having no significant effect on MA currents elicited in Rosette neurons (Figure 3B, rose bars) providing strong evidence that MA currents in Inkblot neurons are largely if not wholly dependent on piezo2. We do not currently know whether Inkblots define a relevant population in vivo, but this is not important for our purpose. The identification of this morphologically distinct population displaying rapid RA currents that depend on piezo2 expression enable us to address the regulation of endogenous piezo2, which would be exceedingly more difficult using a blind approach. Indeed, while Inkblots represent only a subpopulation of small-medium neurons expressing piezo2 (Coste et al., 2010), the ability to identify a native cell population expressing piezo2 enabled us to test whether BK modulated RA MA currents. In all 18 neurons tested, BK (100–1000nM) robustly increased current amplitude (3.6-fold) and τ-inac (1.9-fold) (Figure 3C) compared to vehicle controls which showed a slight rundown and acceleration of τ-inac over 25min (Figures 3C,D, clear vs. solid red boxes). The AUC revealed a dramatic 7.7-fold increase in the presence of BK (Figure 3D, right panel) and partial reversibility during washout under these recording conditions (data not shown). The latency for the BK effect on MA currents was 55±8sec (n=6). These effects are remarkably similar to modulation of recombinant piezo2 in HEK293T cells. Also similar to Piezo2+BDKRB2-HEK cells was the lack of correlation between the magnitude of the RA currents and the change in holding current at -80mV during the BK-induced effect on Inkblots (data not shown). HOE-140 blocked the BK-induced modulation, indicating that endogenous BDKRB2 were responsible for the observed effects (Figure 3D, red hatched).

We reasoned that if the mechanisms underlying piezo2 regulation in Inkblots were similar to those in Piezo2+BDKRB2-HEK cells, then PKA and PKC inhibitors should reduce BK effects on native MA currents. Indeed, the combination of antagonists abrogated the BK-induced facilitation (Figure 3E) suggesting the heterologous system could recapitulate native neuronal mechanisms. The molecular identity of the downstream target(s) leading to augmented piezo2 activity is unknown and may include piezo2 (Coste et al., 2012), piezo2-associated proteins or other signaling components. Piezo2 is encoded by >2500 amino acids and contains putative consensus PKA and PKC phosphorylation sites. Of these 39 sites, four putative PKC sites are likely to be in transmembrane domains according to the Kyte-Doolittle hydrophobicity prediction (Figure S2). Site directed mutagenesis of these sites and/or the acquisition of an efficient antibody will enable testing the hypothesis that piezo2 is directly phosphorylated by BDKRB2 activation.

These data indicate that piezo2-dependent RA channel activity is enhanced by a potent inflammatory algogen through activation of PKA and PKC in both heterologous expression

systems and native sensory cells. We suggest that up-modulation of piezo2 activity contributes, at least in part, to inflammatory mechanical hyperalgesia. Since piezo2 constitutive knockout mice die at birth (data not shown) and attempts at RNAi knock down by intrathecal injection of piezo2 siRNA had no effect on transcript levels in the lumbar DRG, definitive in vivo demonstration for a role of piezo2 in BK-induced mechanical hyperalgesia will have to wait for conditional knockout mice. PKA and certain PKC isoforms play important roles in mechanical hyperalgesia (Hucho and Levine, 2007; Khasar et al., 1999a; Khasar et al., 1999b; Koda and Mizumura, 2002). The mechanism described here differs from another model of mechanical hyperalgesia (epinephrine-induced PKCε-mediated) in which the downstream effector of cAMP is EPAC rather than PKA since the BK effects observed here require PKA activity and neither PI-PLC (Hucho et al., 2005) nor PLD (López De Jesúss et al., 2006) appear to be involved. Inhibition of both kinases is required to block the effects of BK, suggesting the involvement of parallel PKA and PKC pathways. BK-induced mechanical activity in sensory neurons has been observed in a number studies that also implicate cAMP (through an unknown effector) and PKC activation as an underlying mechanism (Dray et al., 1992; Koda and Mizumura, 2002). Although five PKC isoforms have been reported in DRG neurons, BK has been shown to sensitize DRG neurons by translocating PKCε to the membrane (Cesare et al., 1999). In our heterologous system we found that activation of PKA and PKC by co-application of 8-BrcAMP and PMA to Piezo2-HEK cells was less effective at modulating piezo2 than BDKRB2 activation in Piezo2+BDKRB2-HEK cells (compare Figure 2A and Figures 1B,D). However, the BK response was nearly completely blocked by the combination of PKA and PKC inhibitors. Several possibilities could explain this, including higher efficiency of local changes in signaling during BK exposure compared to global increases in PKA and PKC agonists, and involvement of other downstream signaling pathways.

Here we establish a framework for the signal transduction pathway initiated by an inflammatory mediator culminating in hyperactivity of a mechanotransduction channel in mammalian somatosensory neurons. Future work will determine the role of piezo2 in the mechanosensitivity of sensory neurons innervating different targets (e.g., cutaneous, deep tissue and/or visceral) and the underlying molecular mechanisms by which piezo2 MA activity is modulated by intracellular signaling.

Experimental Procedures

All animal protocols were approved by The Scripps Research Institute Animal Subjects Committee in accordance with National Institutes of Health guidelines and public law and all experiments conformed to the relevant regulatory standards. Methods are essentially as described in (Coste et al., 2010) with the following exceptions.

DRG cell culture and selection

DRG neurons from all spinal levels were cultured in NT-4 (50ng/ml) and NGF (100ng/ml) at low density and tested 16–72hr after plating. "[M]edium-sized neuron[s] with very flattened growth cones" were first described in low-density cultures exposed to BDNF (Fig. 2D in (Lindsay, 1988)) and we dub them Inkblots. The following six criteria were used to identify an Inkblot neuron: small-medium diameter (10–37μm) (criterion#1) with 1 to 5 phase dark flattened primary extensions (criterion#2) that do not extend beyond 6 soma diameters (criterion#3), at least one of which partially wraps around the soma (criterion#4). The processes harbor short flattened secondary processes (criterion#5) with a few large varicosities, particularly at branch points (criterion#6). For typical inkblots that were well separated from nearby cells, the apparent number of primary processes was 3±1, the number of branch points was 45±6, and the arbor size (@16–24hr) per soma diameter was 4.5±0.4

(n=6). RA MA characteristics and fold-changes induced by BK were similar in 1day and older cultures; a trend toward smaller MA current amplitude at 2–3days was not significant.

HEK293T cell culture

HEK cells were transiently transfected with 0.6μg piezo2-pSPORT6 cDNA/ml and 0.3μg pHAGE CMG ZsGreen cDNA with or without 1μg/ml human Bdkrb2-pcDNA3.1+ cDNA. Selected cells appeared well attached as single cells or in pairs or in small clusters of up to 5 cells, with 1–2 GFP+ cells/cluster. Cells were maintained at moderate confluence through 14 passages or until their responsiveness to BK was poor when transfected with piezo2 and Bdkrb2 constructs.

Electrophysiology

DRG intracellular solution (in mM): 125K-gluconate, 7KCl, 1CaCl$_2$, 1MgCl$_2$, 10HEPES, 1tetraK-BAPTA, 4Mg-ATP, 0.5Na-GTP (pH 7.3 with KOH). To improve retention of intracellular constituents the resistive whole cell configuration was achieved using the zap function on the amplifier (Multiclamp700A)(Dubin and Dionne, 1993) for access resistances (R$_a$) 12–30MΩ (DRG: 21.9±1.1MΩ (n=42); HEK: 18.1±0.3MΩ (n=371)) that were monitored throughout the experiment. Data were accepted only if R$_a$ was stable. The capacitance was continuously or frequently monitored to identify electrical uncoupling in the presence of BK. Only a single cell per coverslip was tested to avoid tachyphylaxis to BK and pre-exposure to other pharmacological tools.

Mechanical stimulation

We took an approach that enabled comparisons of piezo2-dependent currents over a 20min period after their stabilization (which occurred 5–7min after initiating recordings). Cells were usually challenged with increasing probe displacements in increments of 0.5 or 0.7μm from just below threshold to well above half-maximal response to acquire sigmoidal stimulation-response curves (Figure 1A, inset) to enable the calculation of I$_{max}$ for each cell before, during and after exposure to modulators. Thus, families of currents elicited by increasing stimulus intensity (Figure 1A) were acquired every 1–1.5min to monitor I$_{max}$, and holding current. Control experiments to address tachyphylaxis to mechanical stimuli revealed that responses near I$_{max}$ were similar for single large magnitude displacements and the same displacement after undergoing stimulus-response protocols in 0.7μm increments. Piezo2-dependent currents were stable with interstimulus intervals of 5 or 10sec. Modulators were bath applied only after consistent baseline responses to increasing displacements to >50% I$_{max}$ were observed (for HEK: 7min; for DRG: 5min). Sampling interval: 50μsec; filter: 10KHz.

Statistical analysis

Statistical significance between groups was evaluated using Student's *t*-test or One way ANOVA with Newman-Keuls multiple comparison post hoc test. I$_{max}$ was determined by fitting peak current vs. probe displacement with a sigmoidal dose response with variable slope (GraphPad Prizm 4 (v4.03)) for control (I$_{max(control)}$) and modulator-stimulated currents (I$_{max(mod)}$) and the fold-change calculated as I$_{max(mod)}$/I$_{max(control)}$. τ-inac was determined by fitting the decay phase of currents ~20–50% of I$_{max}$ with a single exponential; fold-change was calculated as τ$_{(mod)}$/τ$_{(control)}$. Currents in the range of ~20–50% I$_{max}$ were averaged over 150msec and the AUC was determined using Clampfit and IGOR Pro 5.04B (V_sum in Wave stats). *Pharmacological* tools are listed in the *Extended Experimental Procedures.*

Supplementary Material

Refer to Web version on PubMed Central for supplementary material.

Acknowledgments

References

Andrew D, Greenspan JD. Peripheral Coding of Tonic Mechanical Cutaneous Pain: Comparison of Nociceptor Activity in Rat and Human Psychophysics. Journal of Neurophysiology. 1999; 82:2641–2648. [PubMed: 10561433]

Bae YS, Lee TG, Park JC, Hur JH, Kim Y, Heo K, Kwak JY, Suh PG, Ryu SH. Identification of a Compound That Directly Stimulates Phospholipase C Activity. Molecular Pharmacology. 2003; 63:1043–1050. [PubMed: 12695532]

Bhave G, Gereau RW. Posttranslational mechanisms of peripheral sensitization. Journal of Neurobiology. 2004; 61:88–106. [PubMed: 15362155]

Bleasdale JE, Thakur NR, Gremban RS, Bundy GL, Fitzpatrick FA, Smith RJ, Bunting S. Selective inhibition of receptor-coupled phospholipase C-dependent processes in human platelets and polymorphonuclear neutrophils. Journal of Pharmacology and Experimental Therapeutics. 1990; 255:756–768. [PubMed: 2147038]

Boada MD, Woodbury CJ. Physiological Properties of Mouse Skin Sensory Neurons Recorded Intracellularly In Vivo: Temperature Effects on Somal Membrane Properties. Journal of Neurophysiology. 2007; 98:668–680. [PubMed: 17537905]

Burgess GM, Perkins MN, Rang HP, Campbell EA, Brown MC, McIntyre P, Urban L, Dziadulewicz EK, Ritchie TJ, Hallett A, et al. Bradyzide, a potent non-peptide B2 bradykinin receptor antagonist with long-lasting oral activity in animal models of inflammatory hyperalgesia. Br J Pharmacol. 2000; 129:77–86. [PubMed: 10694205]

Cesare P, Dekker LV, Sardini A, Parker PJ, McNaughton PA. Specific Involvement of PKC-[epsilon] in Sensitization of the Neuronal Response to Painful Heat. Neuron. 1999; 23:617–624. [PubMed: 10433272]

Coste B, Crest M, Delmas P. Pharmacological Dissection and Distribution of NaN/Nav1.9, T-type Ca2+ Currents, and Mechanically Activated Cation Currents in Different Populations of DRG Neurons. J Gen Physiol. 2007; 129:57–77. [PubMed: 17190903]

Coste B, Mathur J, Schmidt M, Earley TJ, Ranade S, Petrus MJ, Dubin AE, Patapoutian A. Piezo1 and Piezo2 Are Essential Components of Distinct Mechanically Activated Cation Channels. Science. 2010; 330:55–60. [PubMed: 20813920]

Coste B, Xiao B, Santos JS, Syeda R, Grandl J, Spencer KS, Kim SE, Schmidt M, Mathur J, Dubin AE, et al. Piezo proteins are pore-forming subunits of mechanically activated channels. Nature. 2012; 483:176–181. [PubMed: 22343900]

Dai Y, Wang S, Tominaga M, Yamamoto S, Fukuoka T, Higashi T, Kobayashi K, Obata K, Yamanaka H, Noguchi K. Sensitization of TRPA1 by PAR2 contributes to the sensation of inflammatory pain. J Clin Invest. 2007; 117:1979–1987. [PubMed: 17571167]

Djouhri L, Bleazard L, Lawson SN. Association of somatic action potential shape with sensory receptive properties in guinea-pig dorsal root ganglion neurones. The Journal of Physiology. 1998; 513:857–872. [PubMed: 9824723]

Dray A, Patel IA, Perkins MN, Rueff A. Bradykinin-induced activation of nociceptors: receptor and mechanistic studies on the neonatal rat spinal cord-tail preparation in vitro. Br J Pharmacol. 1992; 107:1129–1134. [PubMed: 1334751]

Dubin AE, Dionne VE. Modulation of CI-, K +, and Nonselective Cation Conductances by Taurine in Olfactory Receptor Neurons of the Mudpuppy Necturus maculosus. J Gen Physiol. 1993; 101:469–485. [PubMed: 7685047]

Dubreuil AS, Boukhaddaoui H, Desmadryl G, Martinez-Salgado C, Moshourab R, Lewin GR, Carroll P, Valmier J, Scamps F. Role of T-Type Calcium Current in Identified D-Hair Mechanoreceptor Neurons Studied In Vitro. Journal of Neuroscience. 2004; 24:8480–8484. [PubMed: 15456821]

Hofgaard J, Banach K, Mollerup S, Jørgensen H, Olesen S, Holstein-Rathlou NH, Nielsen M. Phosphatidylinositol-bisphosphate regulates intercellular coupling in cardiac myocytes. Pflugers Archiv European Journal of Physiology. 2008; 457:303–313. [PubMed: 18536930]

Huang J, Zhang X, McNaughton PA. Inflammatory Pain: The Cellular Basis of Heat Hyperalgesia. Curr Neuropharmacol. 2006; 4:197–206. [PubMed: 18615146]

Hucho T, Levine JD. Signaling Pathways in Sensitization: Toward a Nociceptor Cell Biology. Neuron. 2007; 55:365–376. [PubMed: 17678851]

Hucho TB, Dina OA, Levine JD. Epac Mediates a cAMP-to-PKC Signaling in Inflammatory Pain: An Isolectin B4(+) Neuron-Specific Mechanism. The Journal of Neuroscience. 2005; 25:6119–6126. [PubMed: 15987941]

Kennedy CR, Proulx PR, Hebert RL. Role of PLA2, PLC, and PLD in bradykinin-induced release of arachidonic acid in MDCK cells. AJP - Cell Physiology. 1996; 271:C1064–1072.

Khasar SG, Lin YH, Martin A, Dadgar J, McMahon T, Wang D, Hundle B, Aley KO, Isenberg W, McCarter G, et al. A Novel Nociceptor Signaling Pathway Revealed in Protein Kinase C [epsilon] Mutant Mice. Neuron. 1999a; 24:253–260. [PubMed: 10677042]

Khasar SG, McCarter G, Levine JD. Epinephrine Produces a beta-Adrenergic Receptor-Mediated Mechanical Hyperalgesia and In Vitro Sensitization of Rat Nociceptors. Journal of Neurophysiology. 1999b; 81:1104–1112. [PubMed: 10085337]

Kim SE, Coste B, Chadha A, Cook B, Patapoutian A. The role of Drosophila Piezo in mechanical nociception. Nature. 2012; 483:209–212. [PubMed: 22343891]

Koda H, Mizumura K. Sensitization to Mechanical Stimulation by Inflammatory Mediators and by Mild Burn in Canine Visceral Nociceptors In Vitro. Journal of Neurophysiology. 2002; 87:2043–2051. [PubMed: 11929922]

Leeb-Lundberg LMF, Marceau F, Müller-Esterl W, Pettibone DJ, Zuraw BL. International Union of Pharmacology. XLV. Classification of the Kinin Receptor Family: from Molecular Mechanisms to Pathophysiological Consequences. Pharmacological Reviews. 2005; 57:27–77. [PubMed: 15734727]

Lewin GR, Moshourab R. Mechanosensation and pain. Journal of Neurobiology. 2004; 61:30–44. [PubMed: 15362151]

Lindsay RM. Nerve growth factors (NGF, BDNF) enhance axonal regeneration but are not required for survival of adult sensory neurons. Journal of Neuroscience. 1988; 8:2394–2405. [PubMed: 3249232]

López De Jesúss M, Stope MB, Weernink PAO, Mahlke Y, Börgermann C, Ananaba VN, Rimmbach C, Rosskopf D, Michel MC, Jakobs KH, et al. Cyclic AMP-dependent and Epac-mediated Activation of R-Ras by G Protein-coupled Receptors Leads to Phospholipase D Stimulation. Journal of Biological Chemistry. 2006; 281:21837–21847. [PubMed: 16754664]

McCarter GC, Reichling DB, Levine JD. Mechanical transduction by rat dorsal root ganglion neurons in vitro. Neuroscience Letters. 1999; 273:179–182. [PubMed: 10515188]

Mizumura K, Sugiura T, Katanosaka K, Banik R, Kozaki Y. Excitation and sensitization of nociceptors by bradykinin: what do we know? Experimental Brain Research. 2009; 196:53–65.

Potenzieri C, Brink TS, Pacharinsak C, Simone DA. Cannabinoid Modulation of Cutaneous A-delta Nociceptors During Inflammation. Journal of Neurophysiology. 2008; 100:2794–2806. [PubMed: 18784270]

Powis G, Seewald MJ, Gratas C, Melder D, Riebow J, Modest EJ. Selective Inhibition of Phosphatidylinositol Phospholipase C by Cytotoxic Ether Lipid Analogues. Cancer Research. 1992; 52:2835–2840. [PubMed: 1316230]

Rugiero F, Drew LJ, Wood JN. Kinetic properties of mechanically activated currents in spinal sensory neurons. The Journal of Physiology. 2010; 588:301–314. [PubMed: 19948656]

Steranka LR, Manning DC, DeHaas CJ, Ferkany JW, Borosky SA, Connor JR, Vavrek RJ, Stewart JM, Snyder SH. Bradykinin as a pain mediator: receptors are localized to sensory neurons, and antagonists have analgesic actions. Proc Natl Acad Sci U S A. 1988; 85:3245–3249. [PubMed: 2896357]

Tsunozaki M, Bautista DM. Mammalian somatosensory mechanotransduction. Current Opinion in Neurobiology. 2009; 19:362–369. [PubMed: 19683913]

van Zeijl L, Ponsioen B, Giepmans BNG, Ariaens A, Postma FR, Várnai P, Balla T, Divecha N, Jalink K, Moolenaar WH. Regulation of connexin43 gap junctional communication by phosphatidylinositol 4,5-bisphosphate. J Cell Biol. 2007 Jun 4; 177(5):881–891. [PubMed: 17535964]

Woolf CJ, Ma Q. Nociceptors Noxious Stimulus Detectors. Neuron. 2007; 55:353–364. [PubMed: 17678850]

Highlights

- The algogen bradykinin (BK) enhances mechanically-activated (MA) piezo2 currents

- B2 receptor activation increases piezo2 current amplitude and slows inactivation

- Protein kinase A and protein kinase C inhibition abrogates both BK-induced effects

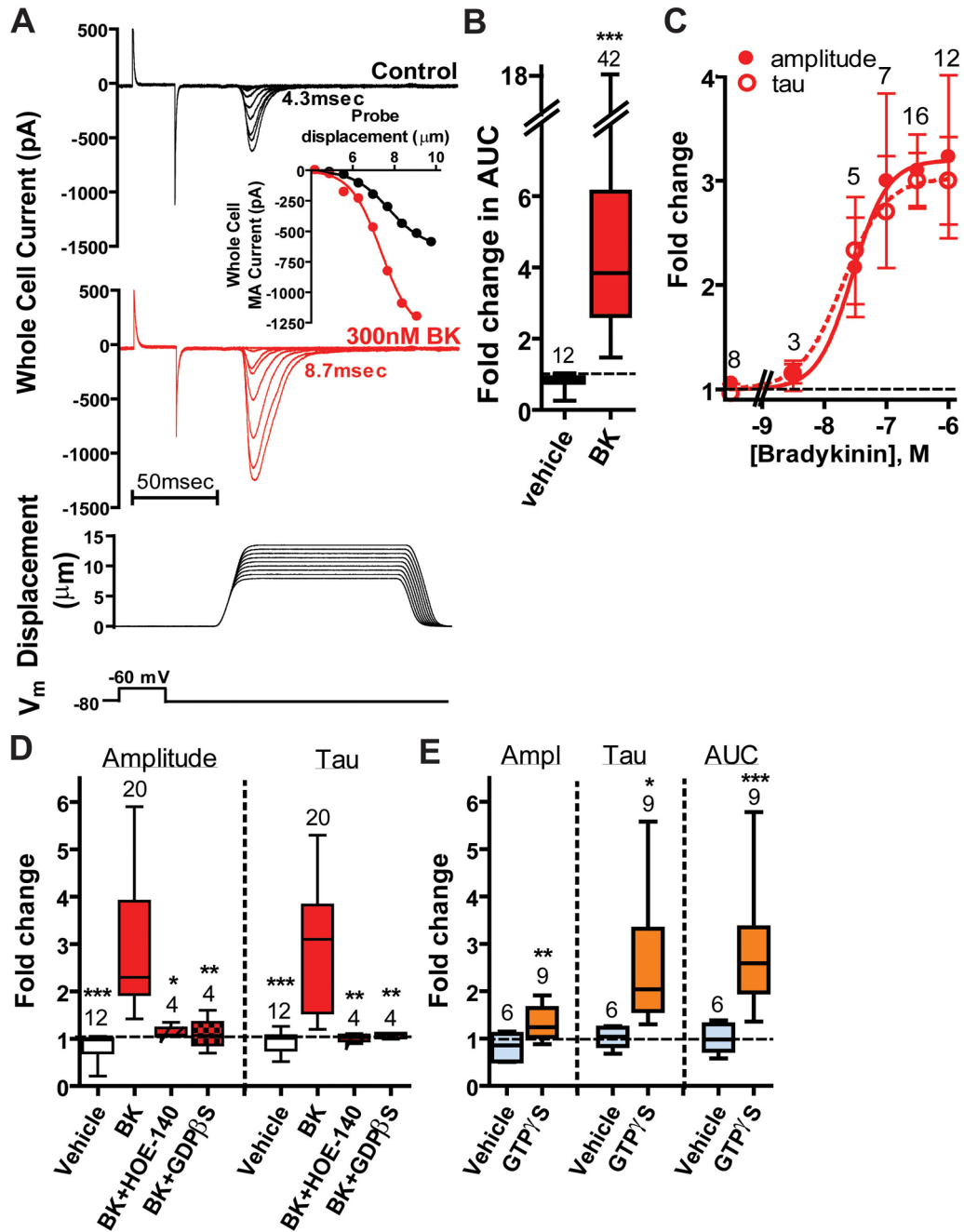- MA currents dependent on piezo2 in DRG neurons are similarly modulated by BK

Figure 1. Piezo2 –induced mechanically activated currents in HEK293T cells are enhanced by bradykinin BDKRB2 and G protein activation

A. MA currents recorded at -80mV in transiently transfected Piezo2+BDKRB2-HEK cells as a function of probe displacement intensity before (black) and during (red) exposure to 300nM BK. Below: ramp (1µm/msec)-and-hold mechanical stimulation protocol. Inset: stimulus-response curves before (black) and during BK exposure (red). **B.** AUC is 6-fold larger in Piezo2+BDKRB2-HEK cells challenged with BK (red bar) compared to vehicle-treated cells (p<0.0001). Fold-change was determined for individual cells as the value in the presence of BK normalized to that prior to BK exposure. Data are presented as box and whiskers plots in which the bottom and top of the box are the 25th and 75th percentile

(lower and upper quartiles, respectively), the band near the middle of the box is the median, and the ends of the whiskers represent the minimum and maximum of all the data. Initial values used to calculate fold-changes are shown in Table S1. **C.** The increase in piezo2 current amplitude and τ-inac ("tau") by BK (plotted as fold-change) is concentration dependent (EC_{50}: 28 nM (95% confidence interval (%CI): 6–140nM) and 20 nM (%CI: 4–100nM), respectively). **D.** Fold-changes are shown for piezo2-dependent current amplitude (left) and τ-inac (right) during application of vehicle only (clear bars), BK (red bars), BK together with H0E-140 after 5min pre-incubation in HOE-140 (red hatched bars), and BK 10min after intracellular perfusion with 667µM GDPβS-3Li (red stippled bars). Similar changes in response to BK were observed for BK in the presence of the vehicles DMSO (0.3%), internal LiCl (2mM), and ethanol (0.1%) for 5–10min and values are combined (red bars). Application of BK at 100, 300 and 1000nM produce similar results and data are combined. *P<0.05;**P<0.01;*** P<0.001 compared to BK; One way ANOVA with Newman-Keuls multiple comparison post hoc test. **E.** Intracellular GTPγS increases piezo2 amplitude, τ-inac and AUC compared to vehicle (2mM LiCl) in Piezo2-HEK cells.*P<0.05;**P<0.01;***P<0.005 using Student's *t*-test. The number of individual cells tested is shown above each bar. See also Table S1.
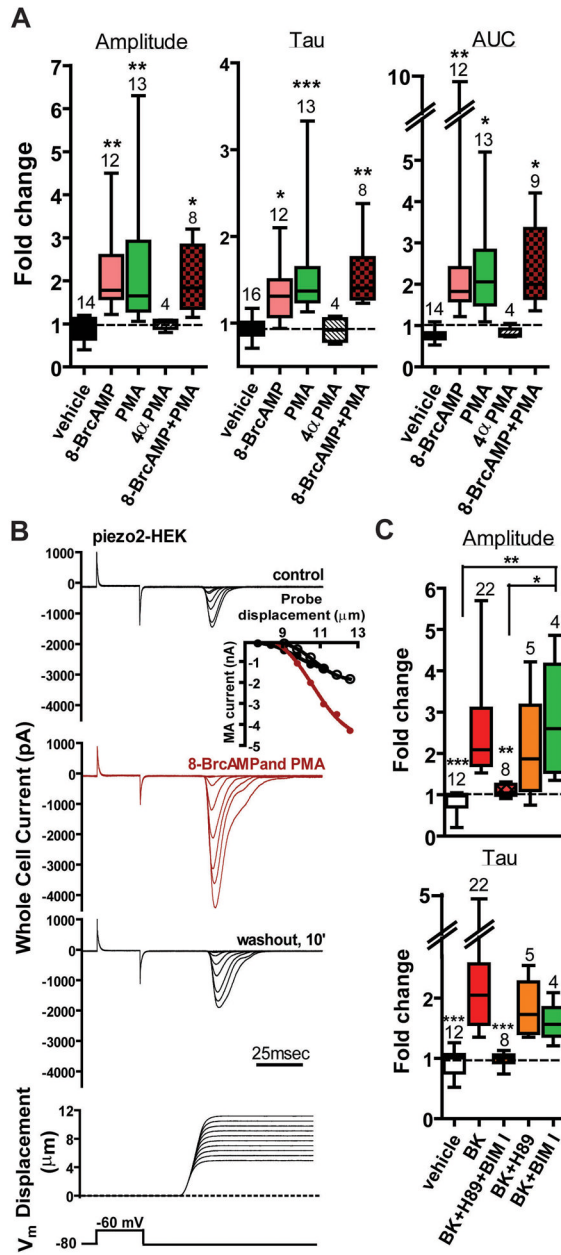
Figure 2. PKA and PKC enhance piezo2-dependent currents

A. Piezo2 MA current amplitude, time course of decay and AUC in Piezo2-HEK cells are enhanced by 8-BrcAMP (100–300μM; pink bars) and PMA (1μM; green bars), but not the inactive congener 4αPMA (1μM; hatched bars). Effects during application of both agonists together were not significantly different than either agonist alone.*P<0.05;**P<0.01 ;***P<0.01 compared to vehicle; One way ANOVA with Newman-Keuls multiple comparison post hoc test. **B.** Recordings showing modulation of piezo2-dependent currents by 8-BrcAMP and PMA. Inset : Peak current-displacement curves for control (black), presence of both agonists (red) and washout (open circles). **C.** Combined inhibition of PKA (H89, 10μM) and PKC (BIM I, 1μM) (red hatched bars), but not H89 (orange bars) or BIM I (green bars) alone, abrogated BK effects on both MA amplitude (top) and τ-inac (bottom) in Piezo2+BDKRB2-HEK cells.*P<0.01;**P<0.001

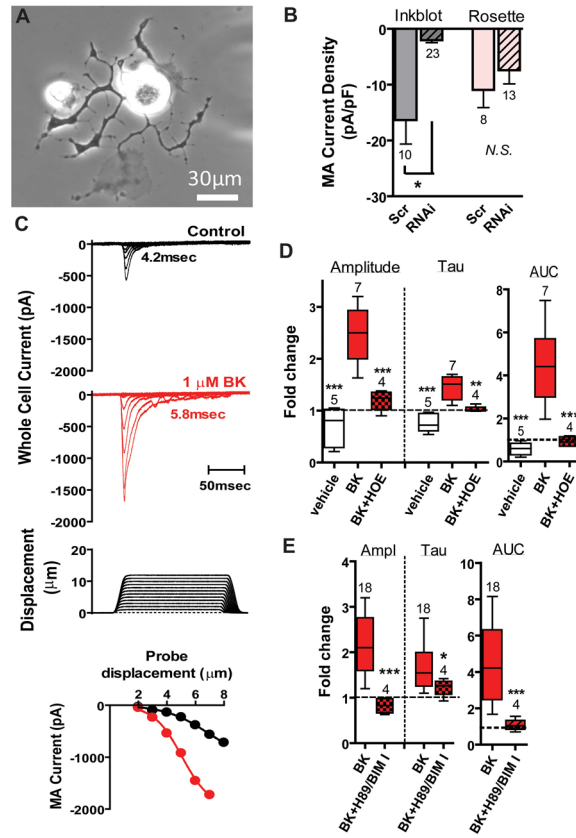compared to BK; One way ANOVA with Newman-Keuls multiple comparison post hoc test. See also Table S1 and Figure S1–S2.

Figure 3. Piezo2-dependent currents in a class of DRG neurons are enhanced by endogenous BDKRB2 activation

A. "Inkblot" neuron 1 day after plating in NT-4- and NGF-containing media. **B.** siRNA pool against piezo2 reduces MA current density in Inkblot neurons three days after nucleofection ("RNAi") compared to scrambled ("Scr") controls (grey bars), and has no significant effect on MA current density of Rosette neurons (pink bars). Four separate experiments. **C.** Families of whole cell MA currents elicited by increasing probe displacement before (black) and with BK (1μM) after 5min of exposure (red). τ-inac values are shown. Inset: peak current as a function of displacement. **D.** BK increases amplitude and AUC and prolongs decay time course ("Tau") through activation of endogenous BDKRB2 (red bars) compared to vehicle (clear bars). Cells pretreated with 1–2μM HOE-140 for 5min prior to BK (100–300nM) exposure in the continued presence of HOE-140 significantly suppressed BK effects.**P<0.01; ***P<0.001; One way ANOVA with Newman-Keuls multiple comparison post hoc test. E. PKA and PKC inhibition abolished BK effects on Inkblot neurons. *P<0.05; ***P<0.001 compared to BK using Student's *t*-test. See also Table S1.